SoftwareX 27 (2024) 101854

Contents lists available at ScienceDirect

SoftwareX

journal homepage: www.elsevier.com/locate/softx

Original software publication

KneeBones3Dify: Open-source software for segmentation and 3D reconstruction of knee bones from MRI data

Lucia Maddalena [a,1], Diego Romano [a,1], Francesco Gregoretti [a,*], Gianluca De Lucia [a], Laura Antonelli [a], Ernesto Soscia [b], Gabriele Pontillo [c], Carla Langella [d], Flavio Fazioli [e], Carla Giusti [f], Rosario Varriale [g]

[a] *Institute for High-Performance Computing and Networking, National Research Council, Via P. Castellino 111, Naples, 80131, Italy*
[b] *Institute of Biostructure and Bioimaging, National Research Council, Via Tommaso De Amicis 95, Naples, 80145, Italy*
[c] *Department of Architecture, University of Florence, Design Campus, Via Sandro Pertini 93, Calenzano (FI), 50041, Italy*
[d] *Department of Architecture, University of Naples Federico II, Via Forno Vecchio 36, Naples, 81024, Italy*
[e] *Istituto Nazionale Tumori - IRCCS - Fondazione G. Pascale, Via Mariano Semmola 52, Naples, 80131, Italy*
[f] *Fondazione IDIS - Città della Scienza, Via Coroglio 104, Naples, 80124, Italy*
[g] *Esaote S.p.A., Via Coroglio 57, Naples, 80124, Italy*

ARTICLE INFO

Keywords:
Knee bone segmentation
Python
GPU
Parallel computing
3D bone models for printing

ABSTRACT

KneeBones3Dify is a Python software tool that supports detailed analysis of knee pathologies and preoperative planning for knee replacement surgery based on patient-specific 3D models. It produces printable 3D bones in a stereolithography file format by automatically segmenting the femur, patella, and tibia from high-resolution Magnetic Resonance (MR) images with nearly isotropic voxel dimensions. Our software avoids time-consuming and subjective manual segmentation by specialists, offering an accurate and efficient alternative employing GPU acceleration. We validated the results by computing objective metrics against the ground truth voxel-wise segmentation produced for a 3D MR image by specialists, who also confirmed the reconstruction accuracy qualitatively. KneeBones3Dify and annotated data are publicly available, enabling broader research and clinical practice use.

Code metadata

Current code version	v1.0
Permanent link to code/repository used for this code version	https://github.com/ElsevierSoftwareX/SOFTX-D-24-00188
Permanent link to Reproducible Capsule	
Legal Code License	GPL-3.0 license
Code versioning system used	Git
Software code languages, tools, and services used	Python
Compilation requirements, operating environments & dependencies	OS: Linux Requirements: NumPy, SciPy, scikit–image, SimpleITK, PyVista GPU requirements: CuPy, cuCIM
If available Link to developer documentation/manual	https://github.com/gigernau/KneeBones3Dify/blob/main/README.md
Support email for questions	gianluca.delucia.94@gmail.com

* Corresponding author.
E-mail address: francesco.gregoretti@cnr.it (Francesco Gregoretti).
[1] Co-first authors.

https://doi.org/10.1016/j.softx.2024.101854
Received 26 March 2024; Received in revised form 5 July 2024; Accepted 11 August 2024
Available online 22 August 2024

1. Motivation and significance

The increasing incidence of joint disorders due to factors like aging populations, obesity, and dietary habits has led to a corresponding rise in joint replacement surgeries. In Italy alone, these interventions have grown by more than 5% annually. Accurate preoperative imaging is crucial for optimizing surgical outcomes, prosthesis longevity, and cost-effectiveness in joint replacements.

Fundamental steps in knee preoperative imaging are the segmentation of the main bones (femur, patella, and tibia) in the acquired images and the 3D reconstruction of the bone models, enabling surgeons to visualize patient-specific information and precisely evaluate the optimal size and alignment of the prosthesis relative to the remaining bone structures.

The process of bone segmentation is usually carried out manually by specialists, requires much effort, and results as time-consuming and poorly reproducible. Automatic tools to perform the task are desirable and reliable alternatives to avoid these disadvantages.

The accuracy of the segmentation results strongly relies on the resolution of the acquired medical images. Bone segmentation is typically obtained with Computer Tomography (CT) scan imaging instruments that have high intrinsic resolution but use ionizing radiations. Magnetic Resonance Imaging (MRI) offers a compelling alternative as it is non-invasive for the patient. Compared to CT scans, MR images usually have high intrinsic contrast but lack resolution, particularly on the Z axis for the 2D acquisition, thus impacting the visualization of specific anatomical structures. Despite this limitation, MRI excels at differentiating soft tissues like ligaments, menisci, and tendons due to their consistently low signal intensity (unless damaged). However, fluid and fat signals vary depending on the specific MRI sequence. The acquisition sequence should maintain good intra-structure homogeneity and significant contrast with surrounding tissues (without fat suppression) and provide sufficient Z-axis resolution in 2D acquisitions for optimal bone segmentation.

Here, we present KneeBones3Dify [1], a software tool designed to automatically segment and reconstruct femur, patella, and tibia bones from high-resolution MR images and produce a stereolithography file for 3D model printing. Based on the above considerations, the software has been optimized for 3D steady-state MR images with T2 spin-echo without fat suppression, with almost isotropic voxels. With suitable parameter tuning, it can run on 2D MR scans of type T1 or PD without fat suppression, provided they have a consistent number of slices.

Several commercially available software packages offer automated segmentation and 3D model creation of knee bones. Examples include YourKnee by Rejoint,[2] MyKnee by Medacta[3] and Simpleware AS Ortho by Synopsys.[4] Despite the vast literature on the subject [2–4], open-source software in this domain is primarily focused on cartilage segmentation. Tools like pyKNEEr [5] or ROCASEG (RObust CArtilage SEGmentation) [6] exemplify this trend. While other segmentation software, such as MICO (Multiplicative Intrinsic Component Optimization) [7] and LOGISMOS (Layered Optimal Graph Image Segmentation for Multiple Objects and Surfaces) [8] can be adapted for knee bone segmentation, as demonstrated in [9], this may require additional customization.

Given the limited availability of open-source tools for knee bone segmentation and 3D modeling, we made publicly available the KneeBones3Dify software developed for the MEDIA[5] project, which partially supported this work. The main aim of the project was a dedicated MRI platform intended to acquire accurate anatomical information in short acquisition times for non-invasive, pre-, and postoperative imaging in prosthetic implants. The software has been extensively adopted for testing and tuning the dedicated MRI equipment and for selecting additive technologies for the 3D printing of the knee bones, aimed at providing patient-specific models for tailoring the prostheses. The continuous collaboration with orthopedic specialists and designers provided a feedback mechanism to improve all the project components.

Besides its role in the project, KneeBones3Dify empowers researchers, clinicians, and practitioners to delve deeper into knee structure analysis by enabling accurate and efficient knee bone segmentation. The software facilitates applications in surgical planning, disease diagnosis, and biomechanics, enabling investigations like exploring the correlation between preoperative planning and surgical success. This freely available tool fosters advancements in orthopedic and radiological research.

The user interacts with the software through a graphical user interface (GUI) to select the input MR image and various parameters. The software outputs a 3D model of the segmented bones suitable for 3D printing. To evaluate the segmentation accuracy of our software, we also provide a 3D MR image alongside its corresponding ground truth segmentation, meticulously annotated voxel-wise by an expert radiologist [10]. This allows for objective performance assessment using established metrics.

2. Software description

2.1. Software architecture

KneeBones3Dify is written in Python and exploits NumPy [11], SciPy [12], and scikit-image [13] functions to process data. It harnesses the power of CuPy [14] and cuCIM [15] libraries to deliver GPU-optimized versions of such functions, retaining the ease of use associated with the standard syntax. The software performs the following steps (see Fig. 1):

- Pre-processing: transforms the MR images to a standard view, focuses on the region of interest (ROI), and enhances bone contours.
- Segmentation: separates bone and tissue areas and automatically selects the three main bones (tibia, femur, and patella).
- Post-processing: refines the segmentation results to produce a model suitable for 3D printing.
- 3D model creation: creates a 3D mesh for 3D printing by scaling the segmented volume, extracting the isosurface, and smoothing the mesh.

The pre-processing, segmentation, and post-processing steps exploit GPU-optimized functions, while the 3D model creation code runs on the CPU. The obtained result can be interactively refined by changing any of the input parameters through the KneeBones3Dify GUI (see Section 3), which re-applies the software pipeline starting from the corresponding step.

2.1.1. Pre-processing

Pre-processing aims at (1) setting the same volume view for all the MR images, (2) focusing on the ROI, and (3) highlighting the bone contours.

(1) The original MR images are transformed into their sagittal view, which is the one where the smallest of the bones to be segmented, i.e., the patella, can be better perceived. An example is given in Fig. 2, where we show (a) one of the slices of an axial MR image and (b) its sagittal view.

(2) In the case of knee MR images, interesting image areas are those that include the bones of the patient, thus excluding entire black image regions surrounding the body (see Fig. 2(c)). The ROI is obtained as the smallest subset of the image volume that comprises intensity values greater than a fixed small threshold. This step helps focus on the relevant information provided by data and reduces the computational complexity of subsequent steps.

[2] www.rejoint.life
[3] www.medacta.com
[4] www.synopsys.com
[5] www.linkedin.com/showcase/progetto-media/

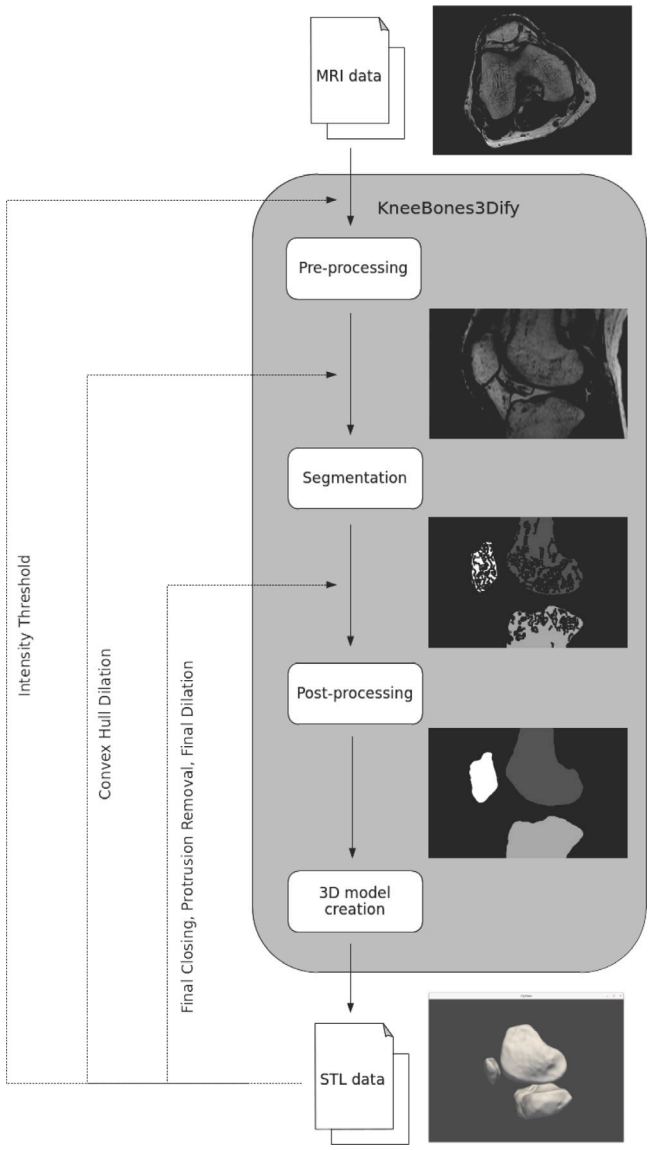

Fig. 1. KneeBones3Dify overview.

(3) As can be observed in Fig. 2, knee bones in the unsaturated MR images appear as gray image areas with dark external contours. This characteristic can be exploited to segment the bones from surrounding knee areas. Therefore, a final pre-processing step is applied to enhance those dark contours (see Fig. 2(d)). This is achieved via the morphological erosion operation, eliminating small bright regions in the image while expanding dark ones, such as the desired dark contours (see Appendix A for details).

2.1.2. Segmentation

Initial thresholding obtained using the Otsu algorithm [16] segments the MR image into two regions, corresponding to two different tissue types: bones and anything else in the knee. The segmentation result for the pre-processed image of Fig. 2(d) is given in Fig. 3(a). Here, white pixels approximately correspond to bone and tissue regions, while black pixels correspond to background areas. The subsequent segmentation steps aim to separate bones and tissue areas and automatically select rough image volumes, including only the three main bones (tibia, femur, and patella). The separation of bones and tissue areas is achieved by erosion (Fig. 3(b)) followed by the elimination of image edges (Fig. 3(c)) from the obtained mask (Fig. 3(d)). Tibia and femur are then chosen among the three connected components (CCs) having the highest volume (shown using different gray levels in Fig. 3(e)) as those having the highest extent (the two CCs in dark and light gray in Fig. 3(e)).

Since the patella has a volume smaller than most of the segmented bones and tissue areas (as shown in Fig. 3(d)), the segmentation algorithm searches for it in a smaller volume, delimited by the femur region on its right and the tibia region in its bottom (Fig. 3(f)). Here, a procedure similar to the one for the tibia and femur is applied to eliminate the edges (Figs. 3(g), (h)) and further separate the remaining regions via erosion (Fig. 3(i)). The patella is selected as the CC having maximum volume (Fig. 3(j)).

Once the three rough areas have been selected (Fig. 4(a)), a slightly finer segmentation is obtained by first dilating their convex hulls (Fig. 4(b)), and then applying a similar segmentation procedure in these areas on a less eroded version of the initial mask. This step allows us to include in the segmented masks most of the boundary areas that were lost in the previous step due to the intense erosion (Fig. 4(c)).

2.1.3. Post-processing

The segmentation procedure succeeds in automatically separating the three bone areas, but still, its results are not yet suitable to produce the final model for the knee bones, as internal areas are only roughly segmented (Fig. 5(a)). Thus, some post-processing steps are required that involve filling in small holes in the bones (Fig. 5(b)), eliminating protrusions (Fig. 5(c)) and filling in bone borders (Fig. 5(d)). Small holes are filled in via a closing morphological operation that first dilates the 3D image and then erodes the dilated image. Small protrusions are eliminated via an opening morphological operation that first erodes the image and then dilates the eroded image. The final filled-in borders are obtained via a dilation morphological operation.

2.1.4. Creation of the 3D model

To create a printable 3D model in the Standard Triangulation Language (STL format), we implemented a procedure that scales the segmented volume to ensure that the print is of the correct dimensions. The printing software uses millimeters for geometry, so it interprets STL files as having units of millimeters. Each unit of the STL corresponds to a voxel. For printing, we need to ensure that each unit of the STL measures 1 mm with specific scaling.

We then extracted the isosurface (mesh) from the segmented volume, a 3D representation of points with equal intensity values.

Finally, we implemented a smoothing mesh procedure. Smoothing is necessary for 3D printing to improve the printed object visual quality and mechanical properties. A smoother mesh can reduce the appearance of visible layer lines and improve the object strength and durability. The procedure removes irregularities and roughness in the 3D model surface by analyzing the local geometry and adjusting the vertex positions to minimize surface distortion. Furthermore, it improves the general quality of the model while maintaining its overall shape and features. This is achieved by applying the Laplacian smoothing that uses the inverse of vertex distances as weights for the discrete version of the operator [17].

2.2. Software functionalities

The functionalities of KneeBones3Dify can be summarized as follows:

- Segmenting the three main knee bones (femur, tibia, patella) from 3D MR images.
- Creating a 3D model of the segmented bones suitable for 3D printing.
- Offering a user-friendly interface for choosing input data and various parameters.
- Allowing the user to change any input parameters after the 3D model creation. Consequently, the software pipeline will restart from the corresponding intermediate state.

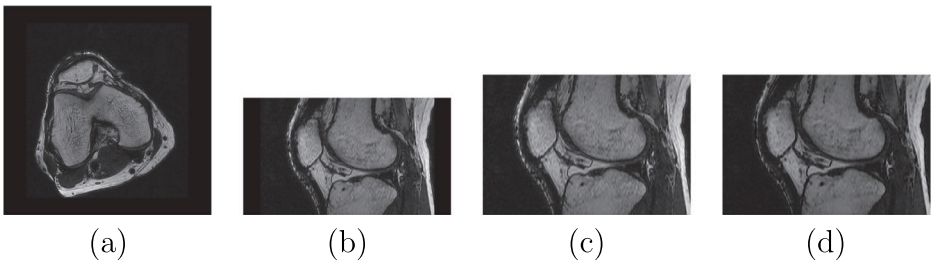

Fig. 2. Pre-processing of an axial MR image of size 512 × 512 × 286: (a) original view; (b) sagittal view; (c) selected ROI; (d) bone contours enhancement.

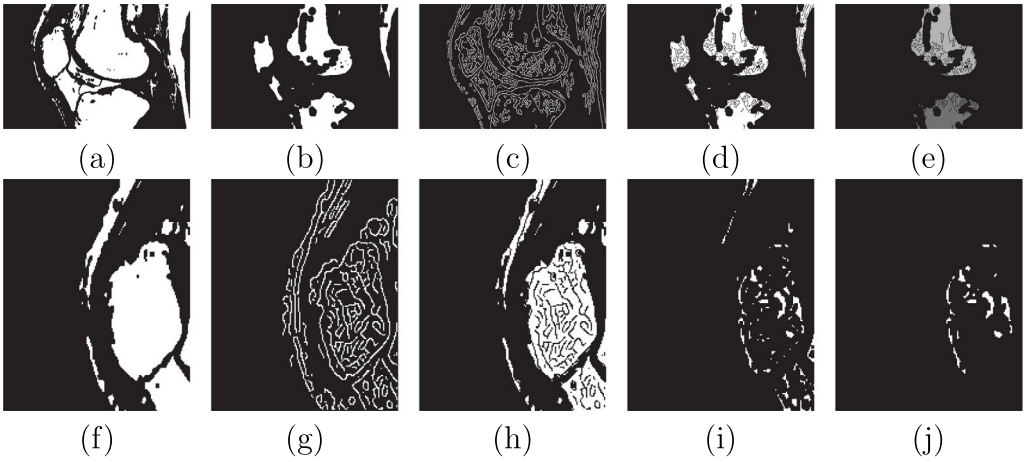

Fig. 3. Segmentation of the pre-processed MR image shown in Fig. 2(d): tibia and femur from (a) to (e), patella from (f) to (j), where (a) initial thresholding; (b) erosion; (c) image edges; (d) elimination of the edges (c) from the eroded mask (b); (e) three 3D connected components having larger volumes (the third one does not appear in the shown slice); (f) subvolume for searching the patella; (g) edges in the subvolume; (h) elimination of the edges; (i) erosion; (j) the connected component of (d) having maximum volume.

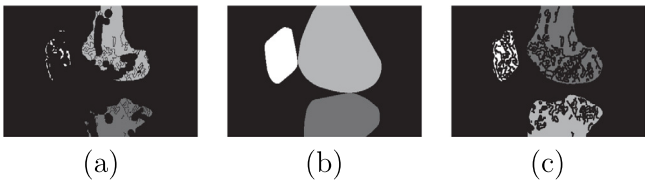

Fig. 4. Segmentation refinement: (a) rough masks of the three bones obtained by segmentation; (b) dilation of the convex hulls; (c) refined segmentation.

Table 1
Performance results of the segmentation obtained using KneeBones3Dify on the example 3D MR image.

DSC	Sens	Spec	VS	AVD
0.939	0.884	1.000	0.939	0.144

3. Illustrative examples

Figs. 2–5 illustrate all the intermediate results of the KneeBones3Dify pipeline (shown in Fig. 1) for the example 3D MR image that we made available [10]. Fig. 6(a) shows the software GUI and Fig. 6(b) provides a 3D view of the reconstructed model.

The segmentation performance has been evaluated against the ground truth voxel-wise segmentation produced by an expert radiologist for the sample MR image, available in [10]. Table 1 reports the obtained performance results in terms of several metrics frequently adopted in the literature [18], summarized in Appendix B: Dice Similarity Coefficient (DSC), Sensitivity (Sens), Specificity (Spec), Volume Similarity (VS), and Average Volume Distance (AVD). All the metrics assume values in [0,1], and the higher, the better, except AVD, for which the lower, the better. These performance values have been computed using the `pymia`[6] evaluation package described in [19]. Fig. 6(c) shows the visual difference between segmentation and ground truth for a single slice.

We further evaluated the reconstructions obtained by KneeBones3Dify through their adoption for 3D printing. For this task, we identified three additive technologies: Fused Deposition Modeling [20], Stereolithography [21], and Polyjet [22]. We chose the printer based on the availability of a dual extruder, proprietary software, and user-friendliness, even for non-experts. We conducted printing tests using the Artillery X2 3D printer[7]. An orthopedic interventionist performed a comparison and preoperative evaluation of 3D-printed knee bone models in terms of size and morphology (Fig. 6(d)). Eighteen knee bone prints (patella, tibia, femur) corresponding to four scans of patients under healthy and pathological conditions were then produced and evaluated. The software creates a single STL file for all bones, but the printer produces them separately. Thus, we assembled three patella-femur-tibia systems using various methods to determine the most suitable solution from an orthopedic application perspective. The connection of bones using semi-flexible spacers proved to be the most suitable solution, closely resembling real ligaments.

4. Impact

KneeBones3Dify has been an essential component of the MEDIA project, extensively used for testing and tuning the dedicated MRI

[6] https://github.com/rundherum/pymia

[7] www.artillery3.com

Fig. 5. Post-processing: (a) refined segmentation of the three bones; (b) closing for filling in bone regions; (c) opening of the tibia and femur for eliminating protrusions; (d) dilating for filling in bone borders.

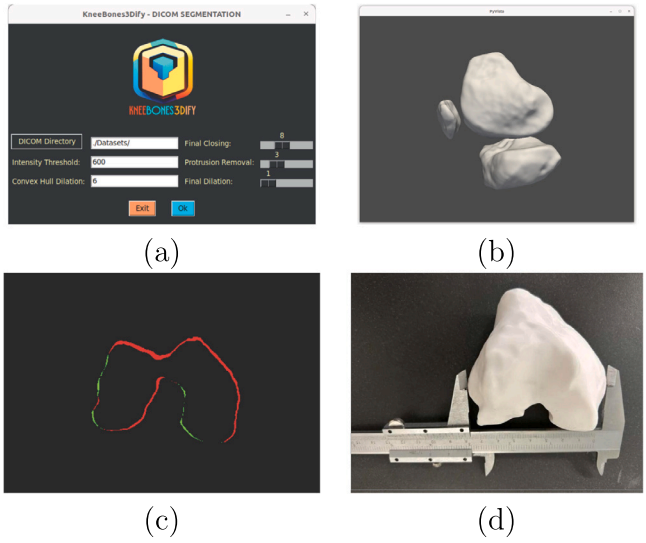

Fig. 6. The KneeBones3Dify software: (a) GUI for input; (b) view of the 3D model constructed from the MR image of Fig. 2; (c) visual difference between segmentation and ground truth: in red, missing voxels; in green, extra voxels; (d) measuring size from the 3D printed model. (For interpretation of the references to color in this figure legend, the reader is referred to the web version of this article.)

equipment intended to acquire accurate anatomical (isotropic) information in short acquisition times and for 3D printing of the knee bones.

4.1. Potential for new and existing research questions

We made KneeBones3Dify publicly available as we believe that it can be used for various research topics, including:

- Developing personalized knee prostheses based on patient-specific MRI data: the 3D printed models accurately represent the unique anatomy of individuals.
- Investigating, based on the 3D printed models, the relationships between knee bone morphology and joint disorders and between preoperative planning accuracy and surgical outcomes.
- Studying the effectiveness of different 3D printing techniques for knee prostheses.

4.2. Impact on daily practice

KneeBones3Dify can improve the workflow for orthopedic surgeons and radiologists and facilitate communication with patients using the reconstructed 3D models, providing a more efficient and radiation-free method for preoperative planning. Physical knee bone models can be highly accurate replicas of real knees, allowing for more realistic and personalized testing of medical devices like joint replacements, implants, and prosthetics. These models can be used to simulate surgeries and test the performance of new medical devices in a controlled environment before they are used on patients.

4.3. Commercialization

Creating physical knee bone models could also lead to future commercial applications across the medical field and beyond: from medical education and surgical planning to consumer wellness and sports science.

5. Conclusions

We proposed and made publicly available KneeBones3Dify, a Python software tool for segmenting the knee bones from MR images and constructing a model for 3D printing. It produces a volume containing the three segmented regions of the bones and the corresponding printable surfaces in a stereolithography file format. The proposed process offers advantages in doctor-patient communication and it could evolve towards the personalization of prostheses by involving manufacturing companies. 3D printing offers versatile and precise solutions, significantly facilitating orthopedic specialists in preoperative evaluations and prosthesis selection.

CRediT authorship contribution statement

Lucia Maddalena: Writing – review & editing, Writing – original draft, Software, Methodology, Data curation, Conceptualization. **Diego Romano:** Writing – review & editing, Writing – original draft, Software, Methodology, Data curation, Conceptualization. **Francesco Gregoretti:** Writing – review & editing, Writing – original draft, Software, Methodology, Data curation, Conceptualization. **Gianluca De Lucia:** Writing – review & editing, Writing – original draft, Validation, Software. **Laura Antonelli:** Writing – review & editing, Writing – original draft, Software, Methodology, Conceptualization. **Ernesto Soscia:** Writing – review & editing, Writing – original draft, Validation, Data curation. **Gabriele Pontillo:** Writing – review & editing, Writing – original draft, Validation. **Carla Langella:** Writing – review & editing, Writing – original draft, Validation. **Flavio Fazioli:** Writing – review & editing, Validation. **Carla Giusti:** Writing – review & editing, Writing – original draft, Validation. **Rosario Varriale:** Writing – review & editing, Writing – original draft, Validation, Data curation.

Declaration of competing interest

The authors declare that they have no known competing financial interests or personal relationships that could have appeared to influence the work reported in this paper.

Data availability

I have shared the link to my data/code within the article.

Acknowledgments

This work has been partially supported by the MEDIA project, co-funded by European Union, PON Research and Competitiveness 2007/2013 PAC, Extract Plan "Research and Innovation" 2015–2017, Development and Cohesion Fund 2014–2020, under the MIUR Directorial Decree n. 713/Ric. 29th October 2010 – Call for the Development/empowerment of High Technology Districts and Public-Private Laboratories and the creation of new Districts and/or new Public-Private aggregations – CALL MIUR PON03. It was also carried out within the activities of the authors from ICAR-CNR as members of the INdAM Research group GNCS and the ICAR-CNR INdAM Research Unit. The authors from ICAR-CNR would like to thank their colleagues, R. Mattiello and S. Sada, for their technical support. Many thanks as well to the late Dr. G. Schmid, without whom this project would never have been possible.

Appendix A. Implementation details

In pre-processing, the erosion applied to the images to enhance the dark contours of the bones (Fig. 2(d)) is a morphological operation where, for each voxel, the value of the corresponding output voxel is the minimum value of all voxels in a neighborhood, defined by a suitable structuring element (SE). Here, the SE is a cube having side 2 voxels.

The initial erosion applied to the segmentation mask (Figs. 3(b) and 3(g)) is obtained using as SE a sphere with radius 7 voxels for tibia and femur and a cube of size 3 voxels for the patella. The edges of the pre-processed MR images (Figs. 3(c) and 3(h)) are obtained slice by slice using the Canny edge detector [23]. The dilation of the convex hulls (Fig. 4(b)) and the mild erosion for obtaining the segmentation (Fig. 4(c)) are obtained using a sphere as SE with a radius of 6 voxels and a square with size 3 voxels, respectively.

The closing, opening, and dilate operations performed for post-processing (Figs. 5(b), (c), (d)) are obtained using as SE a sphere of radius 8, 3, and 1 voxels, respectively. The user can modify the latter SE radiuses and the one used for the convex hull dilation through the GUI.

Finally, the smoothing mesh procedure used to create the 3D model is based on the C code available at [24].

Appendix B. Segmentation metrics

Denoting with A and B the sets of ground truth and segmented voxels, respectively, the Dice Similarity Coefficient (DSC) equals twice the number of elements common to both sets divided by the sum of the number of elements in each set

$$\mathrm{DSC} = \frac{2|A \cap B|}{|A| + |B|} = \frac{2 * TP}{2 * TP + FP + FN}, \tag{1}$$

where TP, FP, and FN indicate the number of voxels correctly segmented as bones, wrongly segmented as bones, and wrongly segmented as background, respectively.

The Sensitivity (Sens), also named Recall or True Positive Rate, gives the accuracy of the bones segmentation

$$\mathrm{Sens} = \frac{TP}{TP + FN}, \tag{2}$$

while the Specificity (Spec), also named True Negative Rate, gives the accuracy of the background segmentation

$$\mathrm{Spec} = \frac{TN}{TN + FP}, \tag{3}$$

where TN indicates the number of voxels correctly segmented as background.

The Volume Similarity (VS) is defined as

$$\mathrm{VS} = 1 - VD = 1 - \frac{|FN - FP|}{2 * TP + FP + FN}, \tag{4}$$

where $VD = \|A| - |B\|/(|A| + |B|)$ is the volumetric distance of A and B, namely the absolute volume difference divided by the sum of the compared volumes.

The Average Volume Distance (AVD) is defined as

$$\mathrm{AVD} = \max(d(A, B), d(B, A)), \tag{5}$$

where $d(A, B)$ indicates the average Housdorff distance of all the points in A and B, given by $d(A, B) = 1/N \sum_{a \in A} \min_{b \in B} \|a - b\|$.

References

[1] De Lucia G, Maddalena L, Romano D, Gregoretti F, Antonelli L. KneeBones3Dify 1.0. Zenodo; 2024, http://dx.doi.org/10.5281/zenodo.10522876.
[2] Ahmed SM, Mstafa RJ. A comprehensive survey on bone segmentation techniques in knee osteoarthritis research: From conventional methods to deep learning. Diagnostics 2022;12(3):611. http://dx.doi.org/10.3390/diagnostics12030611.
[3] Ridhma, Kaur M, Sofat S, Chouhan DK. Review of automated segmentation approaches for knee images. IET Image Process 2021;15(2):302–24. http://dx.doi.org/10.1049/ipr2.12045, URL https://ietresearch.onlinelibrary.wiley.com/doi/abs/10.1049/ipr2.12045.
[4] Li X, Lv S, Li M, Zhang J, Jiang Y, Qin Y, et al. SDMT: Spatial dependence multi-task transformer network for 3D knee MRI segmentation and landmark localization. IEEE Trans Med Imaging 2023;42(8):2274–85. http://dx.doi.org/10.1109/TMI.2023.3247543.
[5] Bonaretti S, Gold G, Beaupre G. pyKNEEr: An image analysis workflow for open and reproducible research on femoral knee cartilage - Validation data. Zenodo; 2019, http://dx.doi.org/10.5281/zenodo.2583184.
[6] Panfilov E, Tiulpin A, Klein S, Nieminen MT, Saarakkala S. Improving robustness of deep learning based knee MRI segmentation: Mixup and adversarial domain adaptation. In: 2019 IEEE/CVF international conference on computer vision workshop. 2019, p. 450–9. http://dx.doi.org/10.1109/ICCVW.2019.00057.
[7] Li C, Gore JC, Davatzikos C. Multiplicative intrinsic component optimization (MICO) for MRI bias field estimation and tissue segmentation. Magn Reson Imaging 2014;32(7):913–23. http://dx.doi.org/10.1016/j.mri.2014.03.010.
[8] Li K, Wu X, Chen DZ, Sonka M. Optimal surface segmentation in volumetric images - A graph-theoretic approach. IEEE Trans Pattern Anal Mach Intell 2006;28(1):119–34. http://dx.doi.org/10.1109/TPAMI.2006.19.
[9] Kashyap S, Zhang H, Rao K, Sonka M. Learning-based cost functions for 3-D and 4-D multi-surface multi-object segmentation of knee MRI: Data from the osteoarthritis initiative. IEEE Trans Med Imaging 2018;37(5):1103–13. http://dx.doi.org/10.1109/TMI.2017.2781541.
[10] Soscia E, Romano D, Maddalena L, Gregoretti F, De Lucia G, Antonelli L. KneeBones3Dify-Annotated-Dataset v1.0.0. Zenodo; 2024, http://dx.doi.org/10.5281/zenodo.10534328.
[11] Harris C, Millman K, van der Walt S, et al. Array programming with NumPy. Nature 2020;585:357–62. http://dx.doi.org/10.1038/s41586-020-2649-2.
[12] Virtanen P, Gommers R, Oliphant TE, et al. SciPy 1.0: Fundamental Algorithms for Scientific Computing in Python. Nature Methods 2020;17:261–72. http://dx.doi.org/10.1038/s41592-019-0686-2.
[13] Van der Walt S, Schönberger JL, Nunez-Iglesias J, Boulogne F, Warner JD, Yager N, et al. scikit-image: image processing in Python. PeerJ 2014;2:e453.
[14] NVIDIA CuPy documentation. 2015, URL https://docs.cupy.dev/en/stable.
[15] NVIDIA cuCIM documentation. 2000, URL https://docs.rapids.ai/api/cucim/stable/.
[16] Otsu N. A threshold selection method from gray-level histograms. IEEE Trans Syst Man Cybern 1979;9(1):62–6. http://dx.doi.org/10.1109/TSMC.1979.4310076.
[17] Belyaev A. Mesh smoothing and enhancing. curvature estimation. Mpi-Inf Mpg de 2006;1–2.
[18] Taha AA, Hanbury A. Metrics for evaluating 3D medical image segmentation: analysis, selection, and tool. BMC Med Imaging 2015;15:29. http://dx.doi.org/10.1186/s12880-015-0068-x.
[19] Jungo A, Scheidegger O, Reyes M, Balsiger F. pymia: A Python package for data handling and evaluation in deep learning-based medical image analysis. Comput Methods Programs Biomed 2021;198:105796. http://dx.doi.org/10.1016/j.cmpb.2020.105796.
[20] Hamzah HH, Shafiee SA, Abdalla A, Patel BA. 3D printable conductive materials for the fabrication of electrochemical sensors: A mini review. Electrochem Commun 2018;96:27–31. http://dx.doi.org/10.1016/j.elecom.2018.09.006.
[21] Hull C. On stereolithography. Virtual Phys Prototyp 2012;7(3):177. http://dx.doi.org/10.1080/17452759.2012.723409.
[22] Patpatiya P, Chaudhary K, Shastri A, Sharma S. A review on polyjet 3D printing of polymers and multi-material structures. Proc Inst Mech Eng C 2022;236(14):7899–926. http://dx.doi.org/10.1177/09544062221079506.
[23] Canny JF. A computational approach to edge detection. IEEE Trans Pattern Anal Mach Intell 1986;8(6):679–98. http://dx.doi.org/10.1109/TPAMI.1986.4767851.
[24] Kroon D-J. Smooth triangulated mesh. 2023, MATLAB Central File Exchange URL https://www.mathworks.com/matlabcentral/fileexchange/26710-smooth-triangulated-mesh.